



# Pyrene and bis-pyrene DNA nucleobase conjugates: excimer and monomer fluorescence of linear and dendronized cytosine and 7-deazaguanine click adducts



Hui Mei<sup>a,b</sup>, Sachin A. Ingale<sup>a,b</sup>, Frank Seela<sup>a,b,\*</sup>

<sup>a</sup>Laboratory of Bioorganic Chemistry and Chemical Biology, Center for Nanotechnology, Heisenbergstraße 11, 48149 Münster, Germany

<sup>b</sup>Laboratorium für Organische und Bioorganische Chemie, Institut für Chemie, Universität Osnabrück, Barbarastrasse 7, 49069 Osnabrück, Germany

## ARTICLE INFO

### Article history:

Received 6 February 2013

Received in revised form 7 March 2013

Accepted 13 March 2013

Available online 18 March 2013

### Keywords:

Nucleoside

DNA

Duplex stability

Click chemistry

Pyrene

Fluorescence

## ABSTRACT

Branched and nonbranched nucleoside pyrene click conjugates were prepared from 5-alkynyl-2'-deoxycytidines using pyrene azide in a copper(I)-catalyzed click reaction. Click chemistry was also applied to oligonucleotides to generate pyrene labeled conjugates with linear or dendronized side chains. While dendronized nucleosides carrying two proximal pyrenes show strong excimer fluorescence, single-stranded oligonucleotides containing two pyrene residues attached to a branched chain display only weak or no excimer emission. Contrary, excimer fluorescence was observed for single-stranded oligonucleotides when proximal alkynylated nucleosides were functionalized. Strong excimer fluorescence was also detected for the 'dC–dG' base pair modified on both nucleobases with pyrene residues, thus having the fluorescent dye in complementary strands. In general, pyrene fluorescence is strongly quenched by the 7-deazaguanine base (charge transfer), while emission of cytosine linked pyrene is not affected. Pyrene interactions were also demonstrated by  $T_m$  increase of DNA duplexes and molecular dynamics simulation.

© 2013 Elsevier Ltd. All rights reserved.

## 1. Introduction

Fluorescent oligonucleotides have been widely used to study nucleic acid structure and function.<sup>1</sup> Among the various fluorophores, pyrene derivatives have attracted notable attention because of their chemical stability, solvatochromic, and tuneable fluorescence, as well as excimer emission.<sup>2</sup> Excimer fluorescence is observed when two pyrene residues are in proximal position.<sup>3</sup> Recently, tripropargylamine pyrene azide click adducts were designed as ratiometric  $Zn^{2+}$  chemosensors.<sup>4</sup>

Excimer emission between pyrene residues is found in double-stranded or single-stranded DNA.<sup>5</sup> Wengel and co-workers showed very efficient interstrand pyrene communication in nucleic acid duplexes based on pyrene-functionalized 2'-amino-LNA residues.<sup>6</sup> Excimer formation by interstrand stacking of pyrene was observed by Häner for non-nucleosidic pyrene derivatives.<sup>7</sup> Kool and co-workers demonstrated excimer formation by pyrene substituted C-nucleosides in single-stranded oligonucleotides.<sup>8</sup>

Kim and co-workers reported on the intrastrand pyrene-stacking in DNA duplexes incorporating 8-ethynylpyrene substituted deoxyadenosines.<sup>9</sup> Highly ordered pyrene stacks on RNA duplexes were constructed by Yamana.<sup>10</sup>

Recently, our laboratory reported on the synthesis and fluorescence properties of 7-deazapurine and 8-aza-7-deazapurine nucleoside and oligonucleotide pyrene click conjugates.<sup>11</sup> In these studies, it was observed that the proximal alignment of pyrene residues in tripropargylamine derivatives (dendronized) causes excimer emission in nucleosides, while no excimer emission was detected for single-stranded and double-stranded oligonucleotides. However, interstrand excimer fluorescence occurred when both strands of duplex DNA were carrying pyrene residues separated by a two base pair distance.<sup>11</sup>

As a continuation of our previous work on pyrene interactions in single-stranded oligonucleotides or duplex DNA, we are now studying pyrene interaction when multiple pyrene residues are linked to the nucleobases of a modified 'dG–dC' base pair or are located in consecutive positions in one strand. For this purpose, the nucleosides **1–4** (Fig. 1) and the oligonucleotide pyrene click conjugates were prepared by the copper-catalyzed Huisgen–Meldal–Sharpless cycloaddition ('click') reaction.<sup>12</sup> The synthesis of nucleoside adducts **1** and **2** is described herein, while compounds **3** and **4** have been reported earlier.<sup>11a</sup> DNA fragments containing either one or two residues of the modified units are

\* Corresponding author. Tel.: +49 (0)251 53 406 500; fax: +49 (0)251 53 406 857; e-mail address: [Frank.Seela@uni-osnabrueck.de](mailto:Frank.Seela@uni-osnabrueck.de) (F. Seela).

URL: <http://www.seela.net>

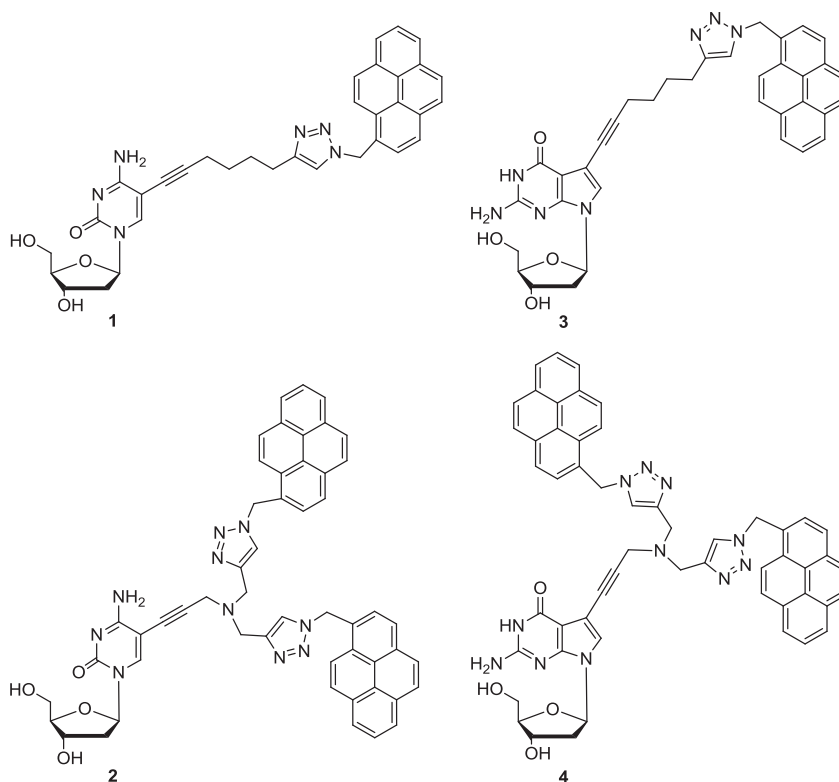


Fig. 1. Structure of nucleoside pyrene mono- and bis-click conjugates.

prepared, and their fluorescence properties are studied with respect to monomer and excimer emission.

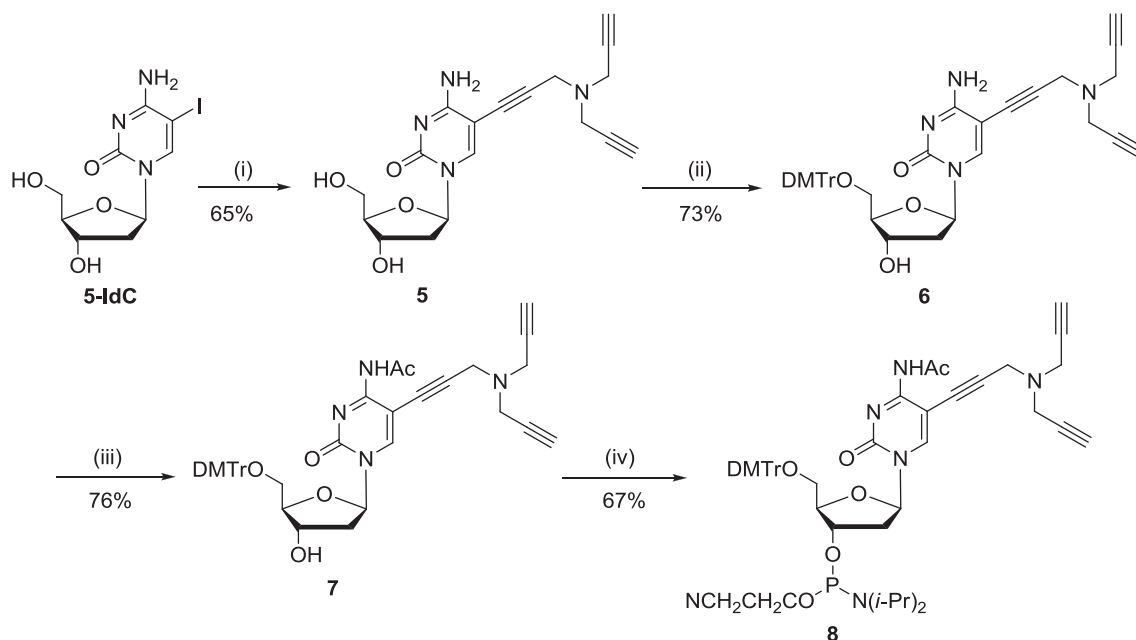
## 2. Results and discussion

### 2.1. Synthesis and characterization of monomers

Nucleoside **5** was synthesized from 5-iodo-2'-deoxycytidine (5-IdC) and tripropargylamine by the Sonogashira cross-coupling

reaction. The reaction was performed in dry DMF in the presence of Et<sub>3</sub>N, [Pd<sup>0</sup>(PPh<sub>3</sub>)<sub>4</sub>], and CuI, with a 10-fold excess of alkyne affording nucleoside **5** in 65% yield. Then, compound **5** was converted to the 5'-O-DMT derivative **6** under standard conditions. Protection of the 4-amino group with an acetyl residue gave **7**, which upon further phosphitylation yielded the phosphoramidite **8** (67%) (Scheme 1).

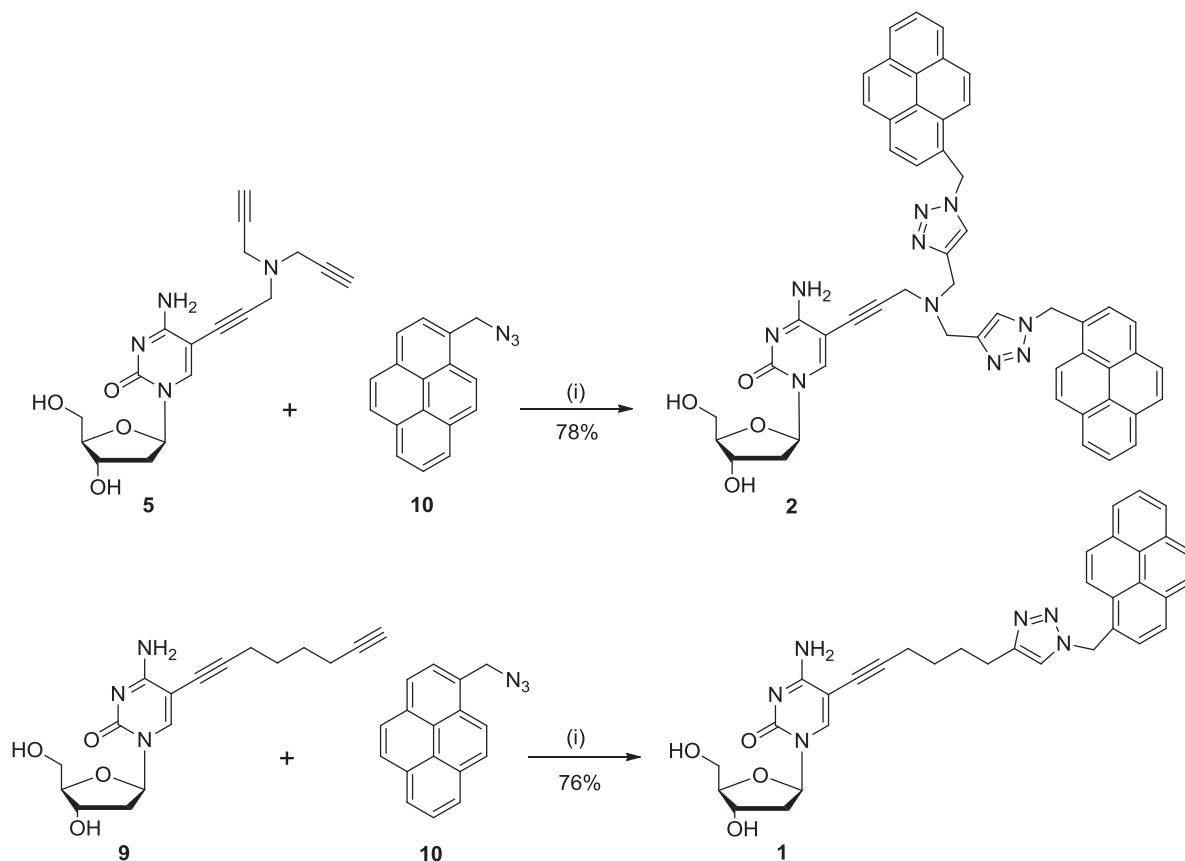
Next, branched nucleoside **5** was functionalized with pyrene azide **10** in a 'double click'<sup>11,13</sup> reaction to give conjugate **2**. A mono



Scheme 1. Synthesis of phosphoramidite **8**. Reagents and conditions: (i) tri(prop-2-ynyl)amine, [Pd(PPh<sub>3</sub>)<sub>4</sub>], CuI, dry DMF, Et<sub>3</sub>N, rt, 12 h; (ii) 4,4'-dimethoxytriphenylmethyl chloride, anhydrous pyridine, rt, 8 h; (iii) acetic anhydride, DMF, rt, 20 h; (iv) 2-cyanoethyl-*N,N*-diisopropylchlorophosphoramidite, anhydrous CH<sub>2</sub>Cl<sub>2</sub>, (*i*-Pr)<sub>2</sub>EtN, rt, 30 min.

click reaction was performed with nucleoside **9** to give **1** (Scheme 2). The branched and nonbranched 7-deaza-2'-deoxyguanosine pyrene click conjugates **3** and **4** have been reported earlier.<sup>11a</sup>

standard protocol (25% aq NH<sub>3</sub>, 60 °C, 16 h). Oligonucleotides were purified before and after detritylation by reversed-phase HPLC.



**Scheme 2.** Synthesis of nucleoside pyrene conjugates **1** and **2**. Reagents and conditions: (i) CuSO<sub>4</sub>·5H<sub>2</sub>O, sodium ascorbate, THF/H<sub>2</sub>O/*t*-BuOH, 3:1:1, rt, 4 h.

All compounds were characterized by elemental analysis, <sup>1</sup>H, <sup>13</sup>C, and <sup>1</sup>H–<sup>13</sup>C-gated-decoupled as well as DEPT-135 NMR spectra (see Supplementary data). The <sup>13</sup>C NMR chemical shifts are listed in Table 1 and were assigned by <sup>1</sup>H–<sup>13</sup>C coupling constants (Supplementary data, Table S2) and DEPT-135 NMR spectra.

In order to introduce the fluorescent pyrene reporter into oligonucleotides, click and double click reactions were performed on oligonucleotides with 1-azidomethylpyrene (**10**) (Scheme 3). The click reaction was carried out at room temperature in an aqueous solution containing *t*-BuOH and DMSO in the presence of a 1:1 complex of

**Table 1**  
<sup>13</sup>C NMR chemical shifts of 2'-deoxycytidine derivatives<sup>a</sup>

	C (2)	C (4)	C (5)	C (6)	C≡C	Triazole	C1'	C2'	C3'	C4'	C5'
<b>5</b>	153.4	164.2	90.1	144.6	89.3, 79.1, 76.6, 76.1	—	85.3	— <sup>c</sup>	70.0	87.4	60.9
<b>6</b>	153.3	164.3	90.3	144.7	89.6, 79.0, 76.1, 76.0	—	85.6 <sup>b</sup>	— <sup>c</sup>	70.6	85.8 <sup>b</sup>	63.7
<b>7</b>	152.5	161.4	93.5	146.8	85.9, 78.9, 76.0, 75.7	—	86.4	— <sup>c</sup>	70.2	87.1	63.4
<b>1</b>	153.6	164.4	95.5	143.6	90.4, 72.1	147.0, 122.2 <sup>b</sup>	85.3	— <sup>c</sup>	70.1	87.4	61.0
<b>2</b>	153.5	164.6	89.9	144.4	89.5, 77.6	143.5, 122.7 <sup>b</sup>	85.4	— <sup>c</sup>	70.0	87.4	60.9

<sup>a</sup> Measured in DMSO-*d*<sub>6</sub> at 298 K.

<sup>b</sup> Tentative.

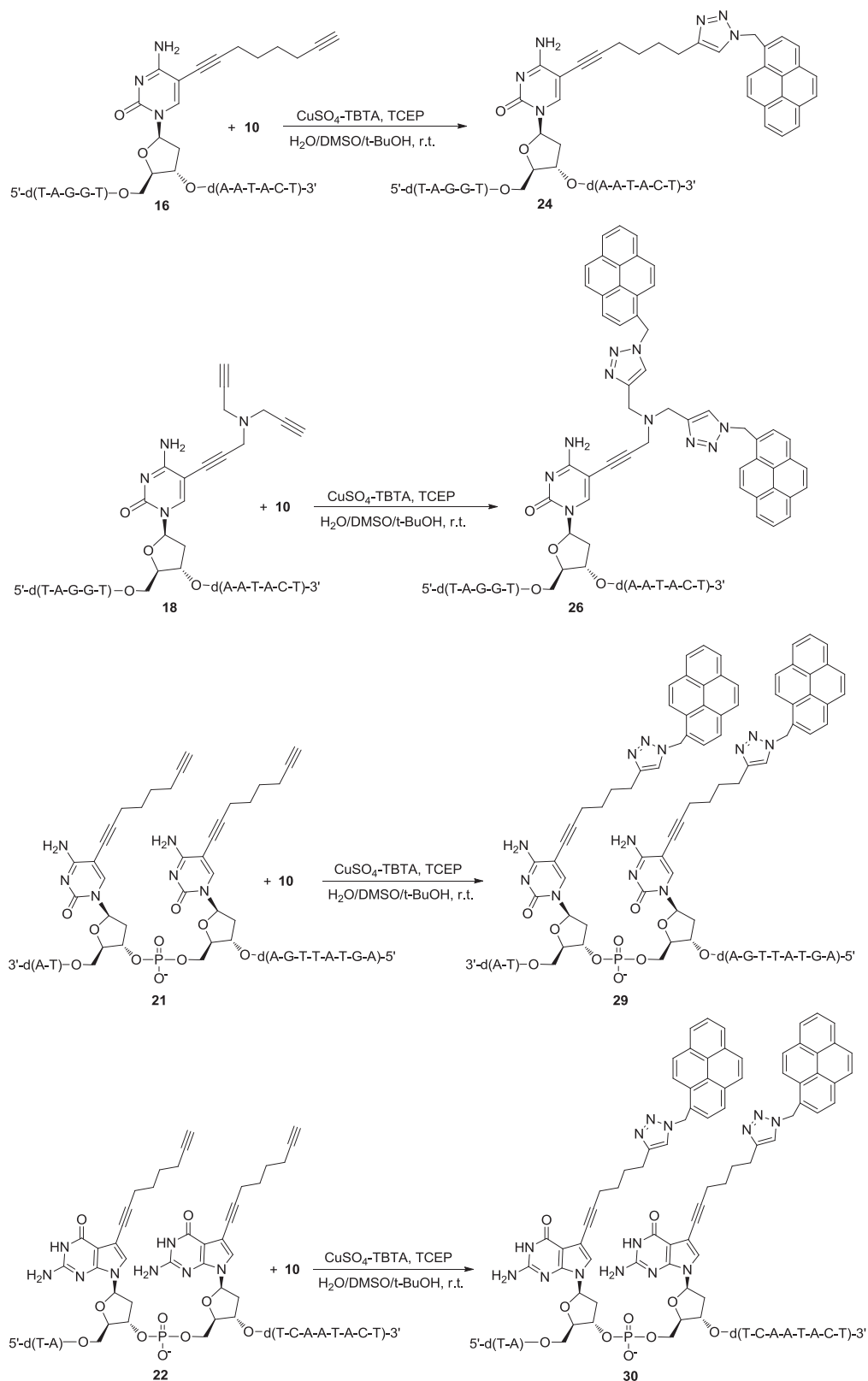
<sup>c</sup> Superimposed by DMSO.

## 2.2. Synthesis and duplex stability of alkynylated oligonucleotides and pyrene conjugates

To evaluate the influence of branched and nonbranched side chain derivatives as well as corresponding pyrene click adducts on DNA duplex stability, a series of oligonucleotides was prepared by solid-phase synthesis. The synthesis was performed in a 1 μmol scale using the newly prepared phosphoramidite **8** as well as reported phosphoramidites **SI–SIII** (for structures see the Supplementary data).<sup>11a,14</sup> After cleavage from the solid support, the oligonucleotides were deprotected following the

CuSO<sub>4</sub>/TBTA [tris((1-benzyl-1*H*-1,2,3-triazol-4-yl)methyl)amine] and TCEP [tris-(2-carboxyethyl)phosphine]. An excess of pyrene azide was used, and the reactions were completed in 15 h. The composition of oligonucleotides was confirmed by MALDI-TOF mass spectrometry. For analytical details see the Supplementary data.

Next, the impact of tripropargylated and octadiynylated cytosine and 7-deazaguanine residues and their click conjugates on duplex stability was studied. For this, the oligonucleotide duplex 5'-d(TAG GTC AAT ACT) (**13**) and 3'-d(ATC CAG TTA TGA) (**14**) was used as reference and the dC and c'<sup>7</sup>G<sub>d</sub> residues were replaced by the branched and nonbranched alkynyl derivatives **5**, **9**, **11**, and **12** (→



**Scheme 3.** Click and double click reactions performed on oligonucleotides with 1-azidomethylpyrene (**10**).

ODNs **15–22**; see Table 2). All oligonucleotide duplexes show melting profiles with a single-phase transition similar to the unmodified duplex **13·14**. The  $T_m$  values are displayed in Table 2. In general, the introduction of the octadiynyl or tripropargyl side chain and modification with pyrene residues has a positive effect on

duplex stability. Even the branched side chains are well accommodated in the major groove of DNA.<sup>11,13</sup> Pyrene dC conjugates show a more pronounced positive effect on duplex stability compared to the 7-deazaguanine adducts (**24·14** and **13·27**, **26·14** and **13·28** as well as **13·29** and **30·14**).

**Table 2**  
 $T_m$  values of oligonucleotide duplexes

Duplexes	$T_m^a$ [°C]	$\Delta T_m^b$ [°C]	Pyrene modified duplexes	$T_m^d$ [°C]	$\Delta T_m^b$ [°C]
5'-d(TAG GTC AAT ACT) ( <b>13</b> ) 3'-d(ATC CAG TTA TGA) ( <b>14</b> )	50	—	5'-d(TAG GTC AAT ACT) ( <b>13</b> ) 3'-d(ATC CAG TTA TGA) ( <b>14</b> )	49 (45) <sup>e</sup>	—
5'-d(TAG GTC AAT ACT) ( <b>13</b> ) 3'-d(AT <b>9</b> CAG TTA TGA) ( <b>15</b> )	53 <sup>c</sup>	+3	5'-d(TAG GTC AAT ACT) ( <b>13</b> ) 3'-d(AT <b>1</b> CAG TTA TGA) ( <b>23</b> )	54.5	+5.5
5'-d(TAG GT <b>9</b> AAT ACT) ( <b>16</b> ) 3'-d(ATC CAG TTA TGA) ( <b>14</b> )	52 <sup>c</sup>	+2	5'-d(TAG GT <b>1</b> AAT ACT) ( <b>24</b> ) 3'-d(ATC CAG TTA TGA) ( <b>14</b> )	59 (55)	+10 (+10)
5'-d(TAG GTC AAT ACT) ( <b>13</b> ) 3'-d(AT <b>5</b> CAG TTA TGA) ( <b>17</b> )	53	+3	5'-d(TAG GTC AAT ACT) ( <b>13</b> ) 3'-d(AT <b>2</b> CAG TTA TGA) ( <b>25</b> )	52.5	+3.5
5'-d(TAG GT <b>5</b> AAT ACT) ( <b>18</b> ) 3'-d(ATC CAG TTA TGA) ( <b>14</b> )	53	+3	5'-d(TAG GT <b>2</b> AAT ACT) ( <b>26</b> ) 3'-d(ATC CAG TTA TGA) ( <b>14</b> )	54.5 (50.5)	+5.5 (+5.5)
5'-d(TAG GTC AAT ACT) ( <b>13</b> ) 3'-d(ATC CA <b>11</b> TTA TGA) ( <b>19</b> )	51 <sup>c</sup>	+1	5'-d(TAG GTC AAT ACT) ( <b>13</b> ) 3'-d(ATC CA <b>3</b> TTA TGA) ( <b>27</b> )	55 <sup>c</sup>	+5
5'-d(TAG GTC AAT ACT) ( <b>13</b> ) 3'-d(ATC CA <b>12</b> TTA TGA) ( <b>20</b> )	50 <sup>c</sup>	0	5'-d(TAG GTC AAT ACT) ( <b>13</b> ) 3'-d(ATC CA <b>4</b> TTA TGA) ( <b>28</b> )	51 <sup>c</sup>	+1
5'-d(TAG GTC AAT ACT) ( <b>13</b> ) 3'-d(AT <b>9</b> <b>9</b> AG TTA TGA) ( <b>21</b> )	55 <sup>c</sup>	+5	5'-d(TAG GTC AAT ACT) ( <b>13</b> ) 3'-d(AT <b>1</b> <b>1</b> AG TTA TGA) ( <b>29</b> )	57 (53)	+8 (+8)
5'-d(TA <b>11</b> <b>11</b> TC AAT ACT) ( <b>22</b> ) 3'-d(ATC CAG TTA TGA) ( <b>14</b> )	53 <sup>c</sup>	+3	5'-d(TA <b>3</b> <b>3</b> TC AAT ACT) ( <b>30</b> ) 3'-d(ATC CAG TTA TGA) ( <b>14</b> )	46.5 (44)	-2.5 (-1.0)
5'-d(TAG GT <b>9</b> AAT ACT) ( <b>16</b> ) 3'-d(ATC CA <b>11</b> TTA TGA) ( <b>19</b> )	52	+2	5'-d(TAG GT <b>1</b> AAT ACT) ( <b>24</b> ) 3'-d(ATC CA <b>3</b> TTA TGA) ( <b>27</b> )	47.5	-1.5
5'-d(TAG GT <b>9</b> AAT ACT) ( <b>16</b> ) 3'-d(ATC CA <b>12</b> TTA TGA) ( <b>20</b> )	52	+2	5'-d(TAG GT <b>1</b> AAT ACT) ( <b>24</b> ) 3'-d(ATC CA <b>4</b> TTA TGA) ( <b>28</b> )	59.5	+10.5
5'-d(TAG GT <b>5</b> AAT ACT) ( <b>18</b> ) 3'-d(ATC CA <b>11</b> TTA TGA) ( <b>19</b> )	52	+2	5'-d(TAG GT <b>2</b> AAT ACT) ( <b>26</b> ) 3'-d(ATC CA <b>3</b> TTA TGA) ( <b>27</b> )	60	+11
5'-d(TAG GT <b>5</b> AAT ACT) ( <b>18</b> ) 3'-d(ATC CA <b>12</b> TTA TGA) ( <b>20</b> )	52	+2	5'-d(TAG GT <b>2</b> AAT ACT) ( <b>26</b> ) 3'-d(ATC CA <b>4</b> TTA TGA) ( <b>28</b> )	57 (52)	+8 (+7)

<sup>a</sup> Measured at 260 nm in 1 M NaCl, 100 mM MgCl<sub>2</sub>, and 60 mM Na-cacodylate (pH 7.0) with 5 μM+5 μM single-strand concentration.

<sup>b</sup>  $\Delta T_m$  was calculated as  $T_m^{\text{modified duplex}} - T_m^{\text{unmodified duplex}}$  using **13**–**14** as comparison.

<sup>c</sup> Lit. value taken from Refs **11a** and **14**.

<sup>d</sup> Measured at 260 nm in 1 M NaCl, 100 mM MgCl<sub>2</sub>, and 60 mM Na-cacodylate (pH 7.0) with 2 μM+2 μM single-strand concentration.

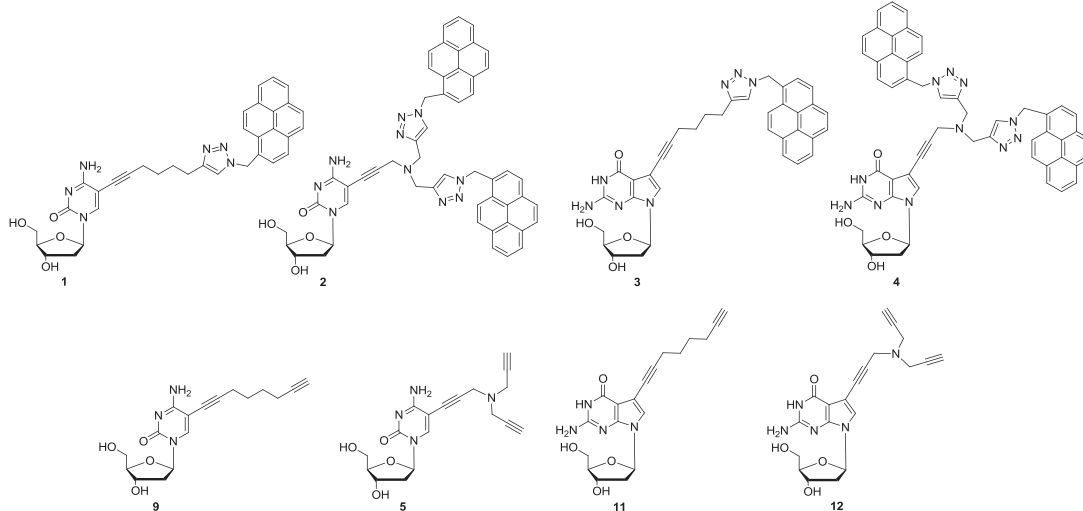
<sup>e</sup> Data in parentheses refer to measurements in 0.1 M NaCl, 100 mM MgCl<sub>2</sub>, and 60 mM Na-cacodylate (pH 7.0) with 2 μM+2 μM single-strand concentration.

When both nucleobases of a dG–dC base pair were functionalized with two, three or even four pyrene residues, the  $T_m$  values changed according to the number of total pyrene residues. Dendronized duplexes bearing two pyrene residues in one chain and at least one in the other strand (**24**–**28**, **26**–**27**, and **26**–**28**) showed significantly increased  $T_m$  values ( $\Delta T_m = +8$ – $11$  °C; **Table 2**). Pyrene stacking might be responsible for this phenomenon. On the contrary, duplex stability decreased slightly compared to **13**–**14**,

when both side chains were bearing just single pyrene residues (**24**–**27**).

### 2.3. Photophysical properties of nucleoside and oligonucleotide pyrene click conjugates

To evaluate the photophysical properties of pyrene adducts, UV/vis and fluorescence spectra of pyrene conjugated nucleosides **1**, **2**,



single-stranded (ss) oligonucleotides (ODNs) **23–30**, and corresponding duplexes (ds) were measured (Figs. 2–6). The UV/vis and fluorescence measurements of nucleosides **1**, **2**, and abasic pyrene click conjugate **31** (4-hexyl-1-methylpyrene-1*H*-[1,2,3]-triazole)<sup>11a</sup> as comparison were performed in MeOH. For solubility reasons, all nucleosides were dissolved first in 1 mL of DMSO and then diluted with 99 mL of MeOH. Identical concentrations of nucleoside pyrene conjugates ( $6.8 \times 10^{-6}$  M) and oligonucleotide pyrene click conjugates ( $2 \times 10^{-6}$  M) were used (for details see Experimental section).

Fig. 2b) as it was observed earlier for the dendronized 7-deazaguanine pyrene adduct **4** or other dendronized pyrene conjugates.<sup>11b</sup> It has been shown that in these cases excimer emission is induced by intramolecular interaction of the pyrene residues.<sup>11b</sup> Contrary to the dC pyrene conjugates **1** and **2**, the 7-deazaguanine pyrene conjugates **3** and **4** show strong quenching of both, monomer and excimer emission, resulting from an intramolecular charge transfer between the dye and the nucleobase ( $c^7G^+ - Py^-$ ).<sup>11,15</sup>

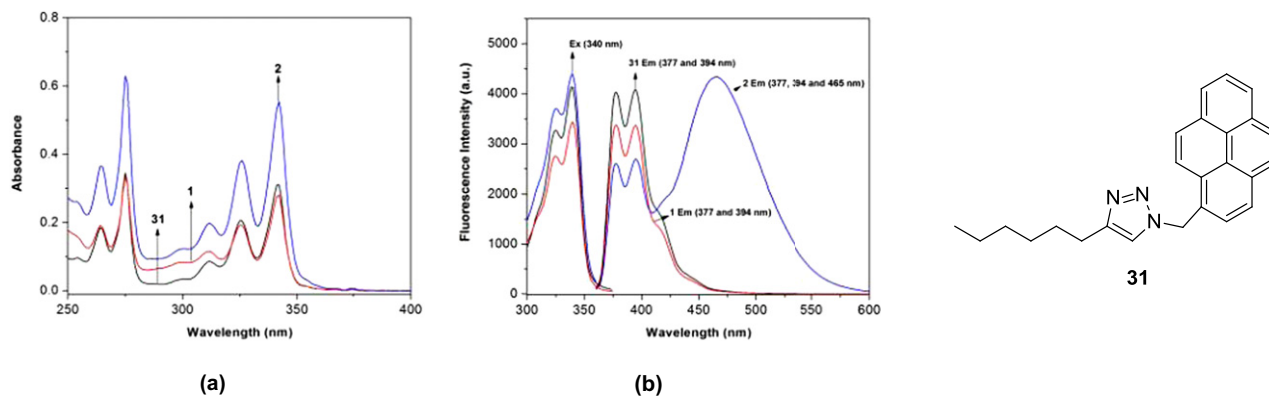


**Fig. 2.** (a) UV/vis spectra of nucleoside conjugates **1**, **2** and non-nucleosidic **31**. (b) Excitation and emission spectra of nucleoside conjugates **1**, **2** and **31**. All measurements were performed in methanol/DMSO (99:1). Excitation wavelength: 340 nm.

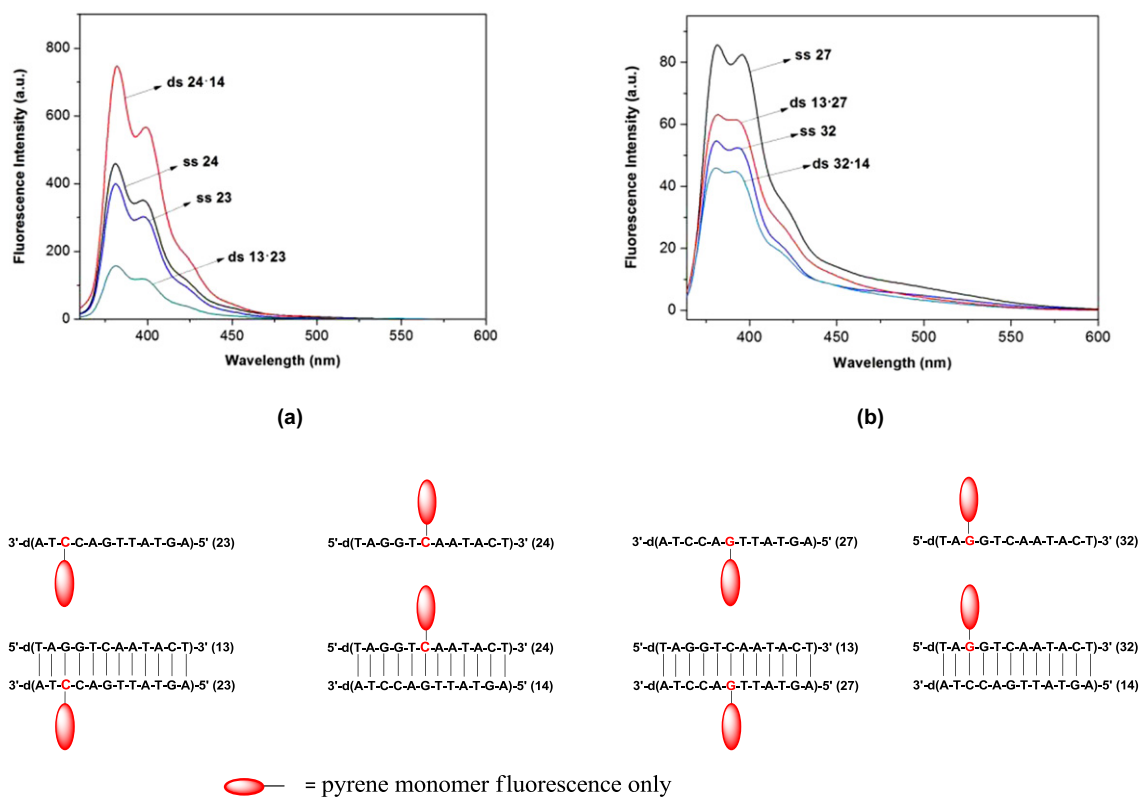


**Fig. 3.** Fluorescence emission spectra of (a) ss **23**, ss **24**, ds **13-23**, and ds **24-14**; (b) ss **27**, ss **32**, ds **13-27**, and ds **32-14**.<sup>11a</sup> All spectra were measured in 1 M NaCl, 100 mM MgCl<sub>2</sub>, and 60 mM Na-cacodylate (pH 7.0) with 2  $\mu$ M of each strand.

**2.3.1. Monomeric cytosine and 7-deazaguanine pyrene click conjugates.** For the dC pyrene conjugate **1**, the fluorescence is only slightly quenched compared to the abasic pyrene click conjugate **31** (Fig. 2b). The dendronized pyrene dC adduct **2** shows monomer emission (377 and 394 nm, Fig. 2b) and excimer emission (465 nm,

**2.3.2. Oligonucleotide pyrene click conjugates.** Subsequently, the photophysical properties of ss and ds oligonucleotides incorporating pyrene nucleoside conjugates were studied. This included the following modifications of ss and ds oligonucleotides: (i) nonbranched pyrene click conjugates, (ii) pyrene click conjugates with two

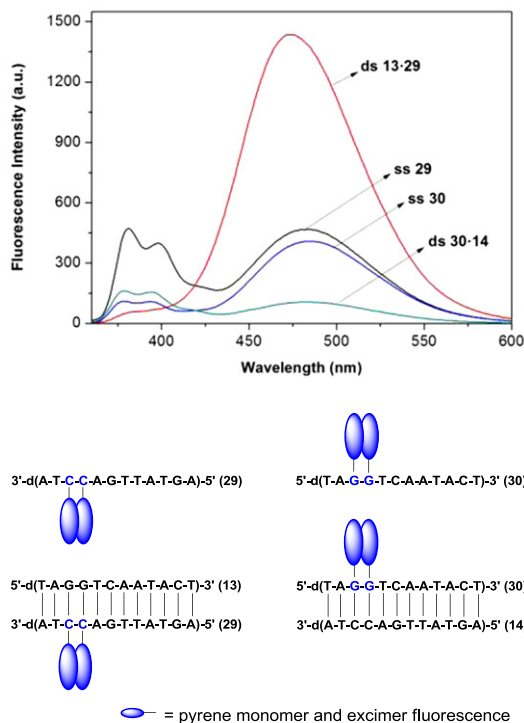


**Fig. 4.** Fluorescence emission spectra of ss **29**, ss **30**, ds **13-29**, and ds **30-14** (2  $\mu$ M of each strand). All spectra were measured in 1 M NaCl, 100 mM MgCl<sub>2</sub>, and 60 mM Na-cacodylate (pH 7.0).

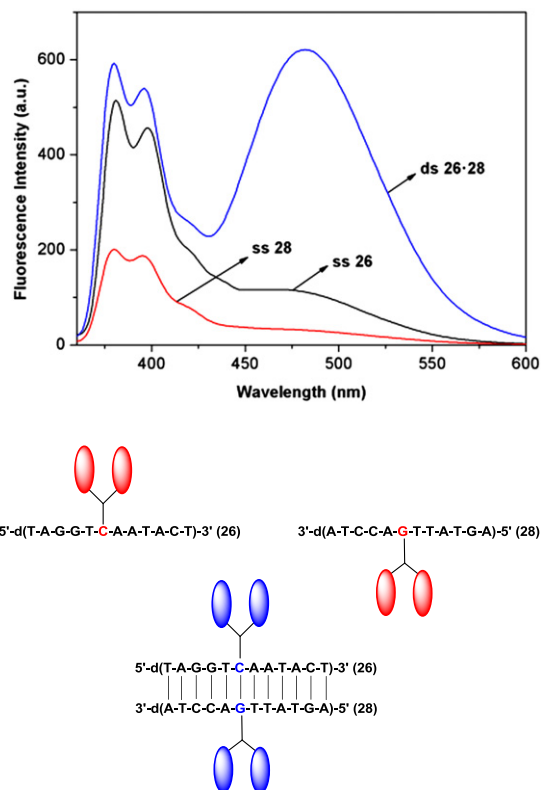


**Fig. 6.** Fluorescence emission spectra of ss **26**, ss **28**, and ds **26-28** (2  $\mu$ M of each strand). All spectra were measured in 1 M NaCl, 100 mM MgCl<sub>2</sub>, and 60 mM Na-cacodylate (pH 7.0).

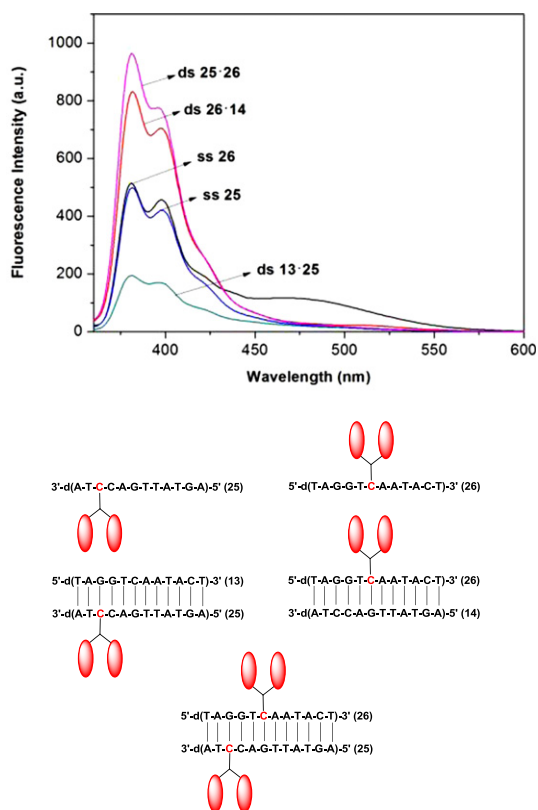


**Fig. 5.** Fluorescence emission spectra of ss **25**, ss **26**, ds **13-25**, ds **26-14**, and ds **25-26** (2  $\mu$ M of each strand). All spectra were measured in 1 M NaCl, 100 mM MgCl<sub>2</sub>, and 60 mM Na-cacodylate (pH 7.0).

consecutive nonbranched dye residues, (iii) branched pyrene click conjugates, (iv) duplexes with pyrene click conjugates as part of a dC–c<sup>7</sup>G<sub>d</sub> base pair. The corresponding fluorescence emission spectra were recorded using an excitation wavelength of 340 nm.

**2.3.3. Single-stranded and double-stranded oligonucleotides with one nonbranched pyrene click conjugate.** Single-stranded oligonucleotides **23** and **24** bearing nonbranched dC pyrene click adduct **1** display typical pyrene monomer emission ( $\lambda_{\text{max}}$  381 nm and 398 nm, Fig. 3a). Depending on the nearest neighbors, the fluorescence intensity slightly varies. This is in line with results reported earlier where the degree of fluorescence quenching by neighboring bases follows the order G>C>T>A.<sup>16</sup> The moderate quenching of pyrene fluorescence is assumed to be a result of a photo-induced electron transfer between neighboring bases (PET). Upon duplex formation, increase or decrease of fluorescence intensity is observed, which can be attributed to the distinct nearest neighbors in the same strand as well as in the complementary strand.<sup>17</sup> Another reason might be the more or less rigid positioning of the pyrene residues in the major groove.

Contrary, the fluorescence of c<sup>7</sup>G<sub>d</sub> pyrene adduct **3** incorporated into ss (**27**, **32**) and ds (**13-27**, **32-14**) oligonucleotides is strongly quenched (Fig. 3b).<sup>11</sup> Different from the dC oligonucleotide pyrene adducts, the observed fluorescence quenching is attributed to charge separation among the nucleobases and pyrene residues, which is strong for 7-deazapurine nucleoside conjugates due to their low oxidation potential.

**2.3.4. Single-stranded oligonucleotides and duplexes containing two consecutive nonbranched nucleoside pyrene residues.** Based on the obtained results, we expanded our studies to oligonucleotides incorporating two consecutive dC or c<sup>7</sup>G<sub>d</sub> pyrene click conjugates in one strand. Both ss oligonucleotides bearing the nonbranched dC

pyrene conjugate **1** or the  $c^7G_d$  adduct **3** (ss **29** and ss **30**) exhibits intrastrand excimer fluorescence (Fig. 4). Similar observations have been made when pyrene residues were linked to the 2'-hydroxyl group of the sugar moiety or were replacing the nucleobase.<sup>8,18</sup> Upon hybridization, ds **13·29** incorporating two dC pyrene adducts shows a significantly increased excimer fluorescence compared to ss **29**, accompanied by a blue shift of the emission maximum of about 9 nm (from 483 nm to 474 nm). On the other hand, the excimer fluorescence of duplex **14·30** bearing two consecutive  $c^7G_d$  pyrene conjugates is strongly quenched compared to the single-strand (ss **30**). These spectroscopic observations indicate that the pyrene residues—as constituents of the dC adduct **1**—are able to adopt a regular and highly organized structure in duplex DNA (ds **13·29**), which allows strong excitonic interactions.<sup>19</sup> Possibly, the pyrene array is located outside of the double helix (see also Fig. 8e).<sup>10a,b</sup> Contrary to this situation, the pyrene rings attached to  $c^7G_d$  in ds **14·30** are now quenched extraordinarily, thus causing the decrease in excimer emission. This assumption is further supported by  $T_m$  measurements (Table 2) and computer modeling (see Section 2.4).

**2.3.5. Branched ss and ds oligonucleotide pyrene click conjugates.** Subsequently, the photophysical properties of ss and ds oligonucleotides bearing branched dC pyrene click conjugate **2** were investigated. Single-stranded oligonucleotides **25** and **26** show slightly higher monomer fluorescence intensities than ss **23** and **24** containing one nonbranched dC pyrene conjugate **1** (Fig. 5). Contrary to ss **23** and **24**, only weak excimer fluorescence was observed for ss **26**, while ss **25** shows no excimer fluorescence. Upon hybridization, monomer fluorescence increased for ds **26·14** compared to ss **26** and no excimer fluorescence was observed anymore. The same is true for ds **25·26** bearing dendronized dC pyrene conjugates even in both strands of the duplex. On the other hand, ds **13·25** showed no excimer fluorescence and decreased monomeric fluorescence in comparison to ss **25**. We assume that the pyrene residues lie apart from each other inside the DNA duplex, preventing excitonic pyrene interactions, and thus excimer fluorescence is not possible. The different tendencies concerning monomeric pyrene fluorescence are probably a result of quenching induced by the nearest neighbors. These findings are in line with the results obtained for oligonucleotides incorporating one nonbranched dC pyrene conjugate **1**.

**2.3.6. Branched and nonbranched pyrene click conjugates attached to the dC- $c^7G_d$  base pair.** Finally, we studied pyrene interactions of a labeled 'dG-dC' base pair, in which both constituents carry at least one pyrene residue. The following combinations were investigated: (i) both constituents are nonbranched pyrene click conjugates (ds **24·27**), (ii) one constituent is a nonbranched conjugate and the other one is a branched pyrene adduct (ds **24·28**, ds **26·27**) and (iii) both constituents are branched pyrene click conjugates (ds **26·28**) (for spectra see Fig. 6 and Fig. S4, Supplementary data). Duplex **26·28** with a dendronized pyrene conjugated dC- $c^7G_d$  base pair (with four pyrene residues) exhibits the strongest excimer fluorescence. Also, ds **26·27** develops significant excimer fluorescence, while for ds **24·28** excimer fluorescence is only minor. Duplex **24·27** containing one pyrene residue in each strand did not show any excimer emission. Our results indicate that it is a prerequisite that at least one strand contains a branched pyrene adduct and the complementary strand carries one pyrene residue to cause excimer fluorescence. Based on our former studies, we anticipate that the pyrene excimer fluorescence is evoked from interstrand communication.

This is supported by temperature dependent fluorescence measurements, which were performed with ds **26·28**. The change of excimer fluorescence during strand separation was monitored at

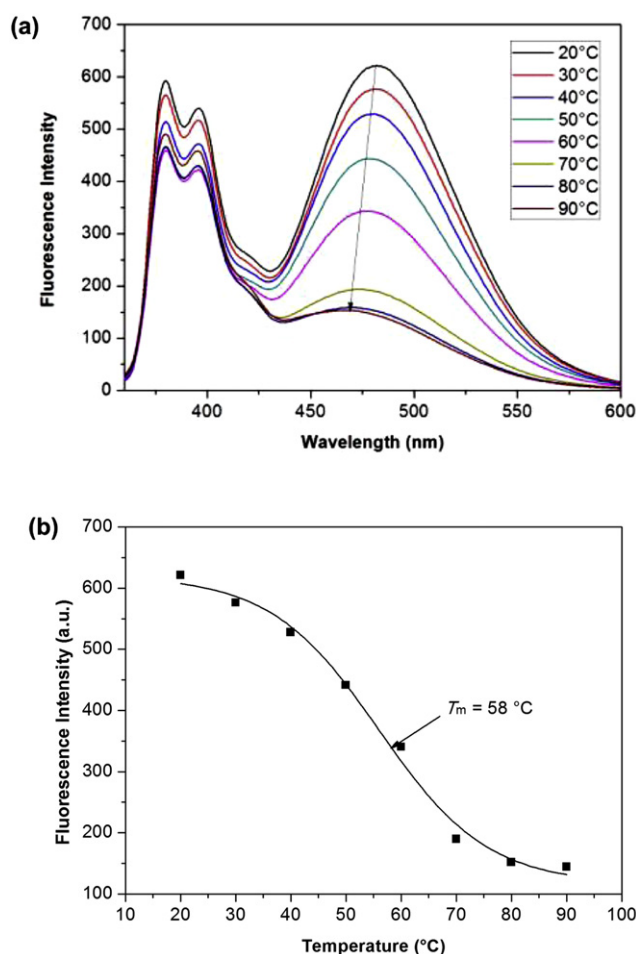


Fig. 7. (a) Temperature dependent fluorescence measurements of ds **26·28**. (b) Temperature depending fluorescence intensity at 480 nm. Fluorescence melting was measured in 1 M NaCl, 100 mM MgCl<sub>2</sub>, and 60 mM Na-cacodylate (pH 7.0) with 2  $\mu$ M+2  $\mu$ M ss concentration.

defined temperatures (Fig. 7a). However, it has to be considered that the fluorescence intensity of a chromophore decreases with increasing temperature. This effect can slightly interfere with the fluorescence change caused by duplex melting.<sup>20</sup>

With increasing temperature, the excimer wavelength was blue shifted from 482 nm to 467 nm. A sigmoidal melting curve was obtained showing a  $T_m$  value of 58 °C (Fig. 7b), which is almost identical to the  $T_m$  value (57 °C) determined by UV measurement (Table 2).

## 2.4. Molecular dynamics simulation

To visualize the pyrene interactions in duplexes, molecular dynamics simulation using AMBER force field were performed on the 12-mer duplexes **26·14** (Fig. 8a,b), **13·29** (Fig. 8c,d) and **30·14** (Fig. 8e,f). The energy minimized molecular structures were built as B-type DNA, and the duplex structure was not significantly disturbed even after introduction of the modifications. Fig. 8a displays duplex **26·14** decorated with two pyrene moieties, in which a central dC-residue is replaced by the branched nucleoside **2**. Surprisingly, the pyrene residues lie far apart from each other, but the spatial arrangement fits to the observation that this duplex exhibits only monomer fluorescence. Another arrangement was obtained for ds **13·29** incorporating two dC pyrene conjugates (**1**) in proximal position. The pyrene residues were located outside the double helix and are perfectly stacking

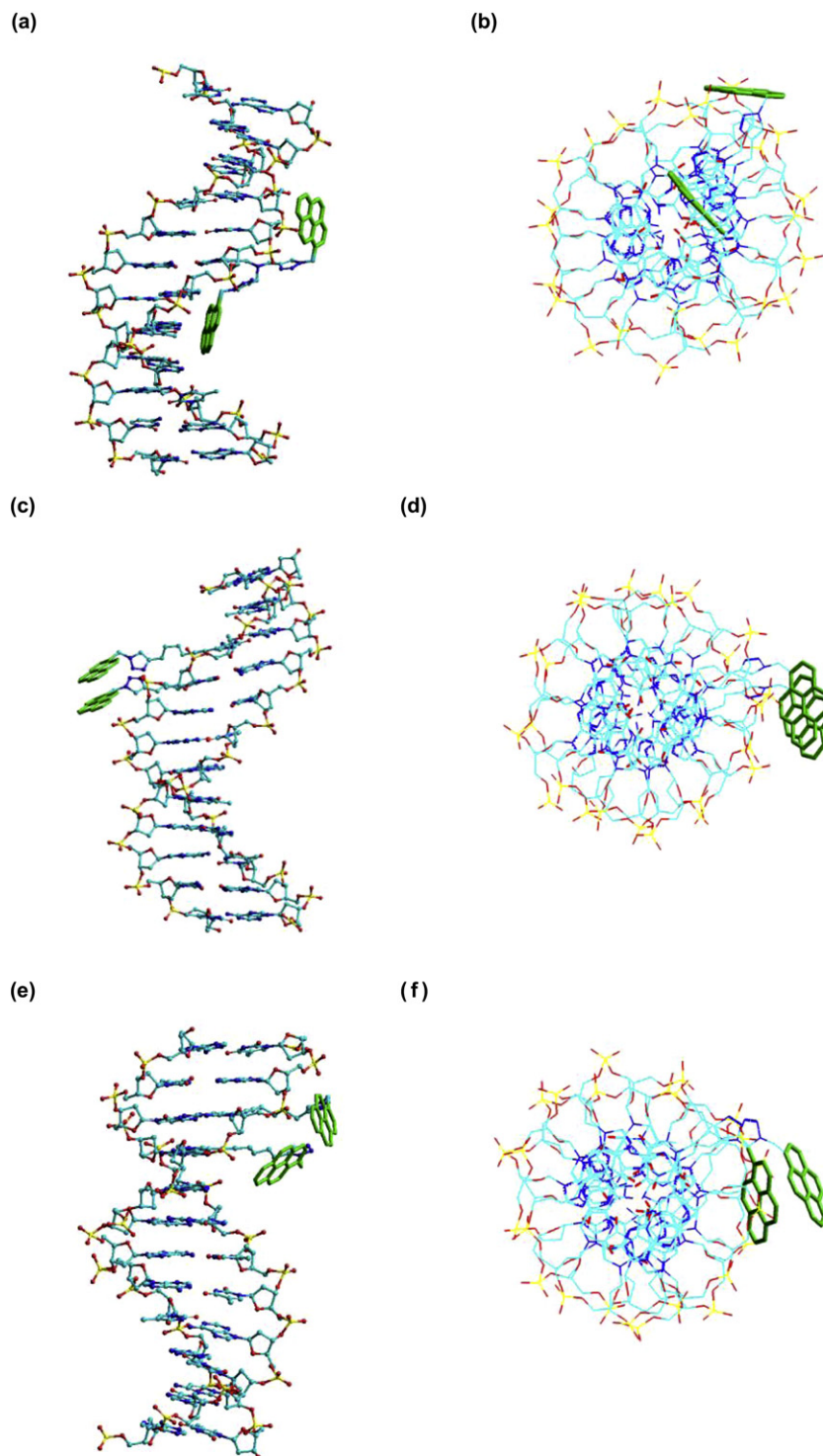


**Fig. 8.** Molecular models of (a) duplex 5'-d(TAG GT2 AATACT) (**26**)-3'-d(ATC CAG TTA TGA) (**14**), side view from the major groove; (b) ds **26-14**, top view; (c) duplex 5'-d(TAG GTC AAT ACT) (**13**)-3'-d(AT1 1AG TTA TGA) (**29**), side view from the major groove; (d) ds **13-29**, top view; (e) duplex 5'-d(TA3 3TC AAT ACT) (**30**)-3'-d(ATC CAG TTA TGA) (**14**), side view from the major groove; (f) ds **30-14**, top view. The models were constructed using Hyperchem 8.0 and energy minimized using AMBER calculations.

(Fig. 8c,d). This is a good example of helical pyrene-array formation along the outside of the DNA duplex and is in line with the observed strong excimer fluorescence (Fig. 4). Interestingly, the situation changes when two  $c^7G_d$  pyrene conjugates (**3**) are placed in proximal position (ds **30-14**; Fig. 8e,f). Now, the two pyrene residues are less favorable positioned to each other, not allowing stacking interactions.

### 3. Conclusion

Pyrene monomer and excimer emission are sensitive to environmental changes in ss and ds DNA. A series of nucleosides and oligonucleotides decorated with pyrenes were synthesized by copper(I)-catalyzed click reaction. The fluorescence is strongly quenched by the 7-deazaguanine base but only weakly affected by cytosine functionalization. Notable excimer fluorescence is

observed for ss-DNA with two consecutive pyrene modifications (ss **29** and ss **30**). While excimer emission strongly increases in duplex DNA when pyrene is linked to the cytosine moiety, it decreases when conjugated to 7-deazaguanine. Stacking of proximal pyrenes outside the DNA helix might provide a strategy to generate  $\pi$ -aromatic arrays as it was already reported for sugar modified pyrene derivatives.<sup>8,18</sup> Pyrene interactions were also demonstrated by  $T_m$  increase and molecular dynamics simulation. Very strong excimer fluorescence occurs when the pyrene residues are part of the  $c^7G_d$ -dC base pair. Here, one strand carries a bis-pyrene moiety while the other strand contains at least one pyrene unit. Our studies performed on nucleoside and oligonucleotide pyrene click conjugates demonstrate the complexity of pyrene interactions in DNA with regard to the sequence motif, base composition and hybridization state. Regarding fluorescence emission, dC click conjugates show superior properties compared to  $c^7G_d$  derivatives, both in single-stranded and double-stranded DNA with linear or dendronized side chains bearing single or bis-pyrene modifications.

## 4. Experimental section

### 4.1. General materials and methods

All chemicals and solvents were of laboratory grade as obtained from commercial suppliers and were used without further purification. Thin-layer chromatography (TLC) was performed on TLC aluminum sheets covered with silica gel 60 F<sub>254</sub> (0.2 mm). <sup>1</sup>H, <sup>13</sup>C, and <sup>31</sup>P NMR spectra were measured with Avance-DPX-300 spectrometer (Bruker, Rheinstetten, Germany) at 300.15 MHz for <sup>1</sup>H, 75.48 MHz for <sup>13</sup>C, and 121.52 MHz for <sup>31</sup>P. The  $J$  values are given in Hertz. The chemical shift of the solvent peak was used for calibration; DMSO: 2.50 ppm for <sup>1</sup>H and 39.50 ppm for <sup>13</sup>C NMR spectra. DEPT-135 and <sup>1</sup>H-<sup>13</sup>C gated-decoupled spectra (<sup>1</sup>H-<sup>13</sup>C coupling constants; Table S2, Supplementary data) were used for the assignment of the <sup>13</sup>C signals. Elemental analyses were performed by Mikroanalytisches Laboratorium Beller (Göttingen, Germany). Reversed-phase HPLC was carried out on a 4 × 250 mm RP-18 (10  $\mu$ m) LiChrospher 100 column with a HPLC pump connected with a variable wavelength monitor, a controller and an integrator. The molecular masses of the oligonucleotides were determined by MALDI-TOF with a Voyager-DE PRO spectrometer (Applied Biosystems) in the linear negative mode with 3-hydroxypicolinic acid (3-HPA) as a matrix or by LC-ESI-TOF (Agilent 1200 Series, Bruker Micro-TOF Q2). The thermal melting curves were measured with a Cary-100 Bio UV/vis spectrophotometer (Varian, Australia) equipped with a Cary thermo-electrical controller. The temperature was measured continuously in the reference cell with a Pt-100 resistor with a heating rate of 1 °C min<sup>-1</sup>. The program MeltWin 3.0 was used for data calculation. UV and fluorescence spectra were recorded on a U-3000 spectrophotometer (Hitachi, Tokyo, Japan) and a F-2500 fluorescence spectrophotometer (Hitachi, Tokyo, Japan). Fluorescence spectra were recorded in the wavelength range between 360 nm and 600 nm. The Hyperchem 7.0/8.0 program package (Hypercube Inc., Gainesville, FL, USA, 2001) was used for molecular modeling to obtain the energy-minimized structure by geometry optimization. The B-type duplex was used as the initial structure, and AMBER force field was used for calculation.

### 4.2. 1-(2-Deoxy- $\beta$ -D-erythro-pentofuranosyl)-5-{3-[di(prop-2-ynyl)amino]prop-1-ynyl}-cytosine (**5**)

To a suspension of 5-iodo-2'-deoxycytidine (1.0 g, 2.83 mmol) and CuI (108 mg, 0.57 mmol) in anhydrous DMF (14 mL) was added successively [Pd(PPh<sub>3</sub>)<sub>4</sub>] (326 mg, 0.28 mmol), anhydrous Et<sub>3</sub>N (720 mg, 7.12 mmol) and tri(prop-2-ynyl)amine (3.7 g, 28.9 mmol). The mixture was stirred at room temperature under nitrogen

atmosphere and allowed to proceed overnight. The reaction mixture was concentrated, and the residue was purified by FC (silica gel, column 15 × 3 cm, CH<sub>2</sub>Cl<sub>2</sub>/MeOH 94:6) affording **5** (0.66 g, 65%) as a yellow solid.  $R_f$ =0.32 (CH<sub>2</sub>Cl<sub>2</sub>/MeOH 9:1). UV/vis (MeOH):  $\lambda_{max}$  ( $\epsilon$ )=238.5 (16,100), 295.5 (8200 mol<sup>-1</sup> dm<sup>3</sup> cm<sup>-1</sup>). <sup>1</sup>H NMR (300 MHz, DMSO-*d*<sub>6</sub>):  $\delta_H$ =1.95–2.17 (m, 2H, 2 × H-2'), 3.23–3.25 (m, 2H, 2 × C≡CH), 3.42, 3.43 (2s, 4H, 2 × CH<sub>2</sub>), 3.51–3.65 (m, 4H, 2 × H-5' and CH<sub>2</sub>), 3.76–3.78 (m, 1H, H-4'), 4.18–4.21 (m, 1H, H-3'), 5.08 (t,  $J$ =5.4 Hz, 1H, 5'-OH), 5.21 (d,  $J$ =4.2 Hz, 3'-OH), 6.10 (t,  $J$ =6.3 Hz, H-1'), 6.80 (s, 1H, NH<sub>a</sub>), 7.73 (s, 1H, NH<sub>b</sub>), 8.17 (s, 1H, H-6). Elemental analysis: calcd (%) for C<sub>18</sub>H<sub>20</sub>N<sub>4</sub>O<sub>4</sub> (356.15): C 60.66, H 5.66, N 15.72; found: C 60.56, H 5.70, N 15.65.

### 4.3. 1-[2-Deoxy-5-O-(4,4'-dimethoxytrityl)- $\beta$ -D-erythro-pentofuranosyl]-5-{3-[di(prop-2-ynyl)amino]prop-1-ynyl}-cytosine (**6**)

Compound **5** (0.32 g, 0.89 mmol) was dried by repeated co-evaporation with anhydrous pyridine (3 × 5 mL). The residue was dissolved in anhydrous pyridine (8 mL) and stirred with 4,4'-dimethoxytrityl chloride (0.40 g, 1.2 mmol) at room temperature for 8 h. The solution was poured into 5% aq NaHCO<sub>3</sub> solution and extracted with CH<sub>2</sub>Cl<sub>2</sub> (3 × 30 mL). The combined extracts were dried (Na<sub>2</sub>SO<sub>4</sub>) and the solvent was evaporated. The residue was purified by FC (silica gel, column 15 × 3 cm, CH<sub>2</sub>Cl<sub>2</sub>/acetone 2:1) to give **6** (0.43 g, 73%) as a colorless solid.  $R_f$ =0.45 (CH<sub>2</sub>Cl<sub>2</sub>/MeOH 94:6). UV/vis (MeOH):  $\lambda_{max}$  ( $\epsilon$ )=236 (36,600), 284 (8750 mol<sup>-1</sup> dm<sup>3</sup> cm<sup>-1</sup>). <sup>1</sup>H NMR (300 MHz, DMSO-*d*<sub>6</sub>):  $\delta_H$ =2.10–2.26 (m, 2H, 2 × H-2'), 3.13–3.28 (m, 8H, 2 × CH<sub>2</sub>, 2 × H-5', 2 × C≡CH), 3.43 (s, 2H, CH<sub>2</sub>), 3.74 (s, 6H, 2 × OCH<sub>3</sub>), 3.91–3.98 (m, 1H, H-4'), 4.21–4.29 (m, 1H, H-3'), 5.31 (d,  $J$ =3.9 Hz, 1H, 3'-OH), 6.12 (t,  $J$ =6.6 Hz, 1H, H-1'), 6.79 (s, 1H, NH<sub>a</sub>), 6.87–7.41 (m, 13H, DMTr-H), 7.79 (s, 1H, NH<sub>b</sub>), 7.92 (s, 1H, H-6). Elemental analysis: calcd (%) for C<sub>39</sub>H<sub>38</sub>N<sub>4</sub>O<sub>6</sub> (658.38): C 71.11, H 5.81, N 8.51; found: C 70.99, H 5.75, N 8.49.

### 4.4. N<sup>4</sup>-Acetyl-1-[2-deoxy-5-O-(4,4'-dimethoxytrityl)- $\beta$ -D-erythro-pentofuranosyl]-5-{3-[di(prop-2-ynyl)amino]prop-1-ynyl}-cytosine (**7**)

To a solution of compound **6** (0.65 g, 0.99 mmol) in DMF (15 mL) was added acetic anhydride (170  $\mu$ L, 1.78 mmol), and the reaction mixture was stirred at room temperature for 20 h. After evaporation of DMF under reduced pressure, the residue was applied to FC (silica gel, column 15 × 3 cm, CH<sub>2</sub>Cl<sub>2</sub>/acetone 3:1). Compound **7** was isolated as colorless foam (0.53 g, 76%).  $R_f$ =0.62 (CH<sub>2</sub>Cl<sub>2</sub>/MeOH 94:6). UV/vis (MeOH):  $\lambda_{max}$  ( $\epsilon$ )=236 (34,500), 283 (8300 mol<sup>-1</sup> dm<sup>3</sup> cm<sup>-1</sup>). <sup>1</sup>H NMR (300 MHz, DMSO-*d*<sub>6</sub>):  $\delta_H$ =2.16–2.25 (m, 1H, H $_{\alpha}$ -2'), 2.28 (s, 3H, CH<sub>3</sub>), 2.34–2.41 (m, 1H, H $_{\beta}$ -2'), 3.13–3.22 (m, 4H, 2 × C≡CH, 2 × H-5'), 3.32–3.33 (m, 4H, 2 × CH<sub>2</sub>), 3.38 (s, 2H, CH<sub>2</sub>), 3.73 (s, 6H, 2 × OCH<sub>3</sub>), 4.02–4.03 (m, 1H, H-4'), 4.24–4.28 (m, 1H, H-3'), 5.37 (d,  $J$ =4.5 Hz, 1H, 3'-OH), 6.06 (t,  $J$ =6.3 Hz, 1H, H-1'), 6.87–7.41 (m, 13H, DMTr-H), 8.24 (s, 1H, H-6), 9.54 (s, 1H, NH). Elemental analysis: calcd (%) for C<sub>41</sub>H<sub>40</sub>N<sub>4</sub>O<sub>7</sub> (700.29): C 70.27, H 5.75, N 7.99; found: C 70.22, H 5.80, N 8.01.

### 4.5. N<sup>4</sup>-Acetyl-1-[2-deoxy-5-O-(4,4'-dimethoxytrityl)- $\beta$ -D-erythro-pentofuranosyl]-5-{3-[di(prop-2-ynyl)amino]prop-1-ynyl}-cytosine 3'-(2-cyanoethyl)-N,N'-diisopropyl phosphoramidite (**8**)

A stirred solution of **7** (0.21 g, 0.30 mmol) in anhydrous CH<sub>2</sub>Cl<sub>2</sub> (10 mL) was pre-flushed with nitrogen and treated with (*i*-Pr)<sub>2</sub>NEt (81  $\mu$ L, 0.48 mmol) followed by 2-cyanoethyl-N,N'-diisopropylphosphoramidochloridite (107  $\mu$ L, 0.48 mmol). After stirring for 30 min at room temperature, the solution was diluted with CH<sub>2</sub>Cl<sub>2</sub> (30 mL) and extracted with 5% aq NaHCO<sub>3</sub> solution (20 mL). The

organic layer was dried over Na<sub>2</sub>SO<sub>4</sub> and evaporated. The residue was purified by FC (silica gel, column 10×2 cm, CH<sub>2</sub>Cl<sub>2</sub>/acetone 15:1) to give **8** (0.18 g, 67%) as a colorless foam. *R*<sub>f</sub>=0.64 (CH<sub>2</sub>Cl<sub>2</sub>/acetone 9:1). <sup>31</sup>P NMR (121 MHz, CDCl<sub>3</sub>): δ<sub>p</sub>=148.53, 149.14.

#### 4.6. Preparation of click conjugate **1** from nucleoside **9** and pyrene azide **10**

Compound **9** (165 mg, 0.50 mmol) and pyrene azide **10** (180 mg, 0.70 mmol) were dissolved in THF/H<sub>2</sub>O/*t*-BuOH (3:1:1, v/v, 8 mL), then sodium ascorbate (200 μL, 0.20 mmol) of a freshly prepared 1 M solution in water was added, followed by the addition of copper(II) sulfate pentahydrate 7.5% in water (166 μL, 0.05 mmol). The reaction mixture was stirred for 4 h at room temperature. The solvent was evaporated, and the residue was purified by FC (silica gel, column 10×3 cm, CH<sub>2</sub>Cl<sub>2</sub>/MeOH 25:1) to give **1** (231 mg, 78%) as a light yellow solid. *R*<sub>f</sub>=0.39 (CH<sub>2</sub>Cl<sub>2</sub>/MeOH 10:1). UV/vis (MeOH): λ<sub>max</sub> (ε)=264.5 (28,200), 275.0 (49,400), 311.5 (17,100), 325.5 (28,600), 341.5 (41,600 mol<sup>-1</sup> dm<sup>3</sup> cm<sup>-1</sup>). <sup>1</sup>H NMR (300 MHz, DMSO-*d*<sub>6</sub>): δ<sub>H</sub>=1.50–1.68 (m, 4H, 2× CH<sub>2</sub>), 1.92–2.01 (m, 1H, H<sub>α</sub>-2'), 2.08–2.16 (m, 1H, H<sub>β</sub>-2'), 2.38 (t, *J*=6.9 Hz, 2H, CH<sub>2</sub>), 2.60 (t, *J*=7.2 Hz, 2H, CH<sub>2</sub>), 3.54–3.59 (m, 2H, 2× H-5'), 3.76–3.79 (m, 1H, H-4'), 4.18–4.20 (m, 1H, H-3'), 5.08 (t, *J*=4.8 Hz, 1H, 5'-OH), 5.20 (d, *J*=4.2 Hz, 1H, 3'-OH), 6.11 (d, *J*=6.6 Hz, 1H, H-1'), 6.32 (s, 2H, pyrene-CH<sub>2</sub>), 6.72 (s, 1H, NH<sub>a</sub>), 7.67 (s, 1H, NH<sub>b</sub>), 7.90 (s, 1H, H-5-triazole), 7.97–8.53 (m, 10H, H-6, pyrene-H). Elemental analysis: calcd (%) for C<sub>34</sub>H<sub>32</sub>N<sub>6</sub>O<sub>4</sub> (588.66): C 69.37, H 5.48, N 14.28; found: C 68.89, H 5.41, N 13.98.

#### 4.7. Preparation of conjugate **2** from nucleoside **5** and pyrene azide **10**

Compound **5** (178 mg, 0.50 mmol) and pyrene azide **10** (360 mg, 1.40 mmol) were dissolved in THF/H<sub>2</sub>O/*t*-BuOH (3:1:1, v/v, 10 mL), then sodium ascorbate (400 μL, 0.40 mmol) of freshly prepared 1 M solution in water was added, followed by the addition of copper(II) sulfate pentahydrate 7.5% in water (332 μL, 0.10 mmol). The reaction mixture was stirred for 4 h at room temperature. The solvent was evaporated, and the residue was purified by FC (silica gel, column 10×3 cm, CH<sub>2</sub>Cl<sub>2</sub>/MeOH 15:1) to give **2** (331 mg, 76%) as a light yellow solid. *R*<sub>f</sub>=0.31 (CH<sub>2</sub>Cl<sub>2</sub>/MeOH 10:1). UV/vis (MeOH): λ<sub>max</sub> (ε)=264.5 (54,300), 275.5 (94,200), 311.5 (29,100), 326.0 (56,300), 342.0 (81,600 mol<sup>-1</sup> dm<sup>3</sup> cm<sup>-1</sup>). <sup>1</sup>H NMR (300 MHz, DMSO-*d*<sub>6</sub>): δ<sub>H</sub>=1.95–2.17 (m, 2H, 2× H-2'), 3.51–3.71 (m, 6H, 2× CH<sub>2</sub>, 2× H-5'), 3.78–3.79 (m, 1H, H-4'), 4.20 (m, 1H, H-3'), 5.09 (t, *J*=4.5 Hz, 1H, 5'-OH), 5.23 (d, *J*=3.6 Hz, 1H, 3'-OH), 6.12 (t, *J*=6.3 Hz, 1H, H-1'), 6.33 (s, 4H, 2× pyrene-CH<sub>2</sub>), 7.13 (s, 1H, NH<sub>a</sub>), 7.84 (s, 1H, NH<sub>b</sub>), 7.94, 7.97 (2s, 2H, 2× H-5-triazole), 8.06–8.50 (m, 19H, H-6, pyrene-H). Elemental analysis: calcd (%) for C<sub>52</sub>H<sub>42</sub>N<sub>10</sub>O<sub>4</sub>·H<sub>2</sub>O (870.95): C 70.26, H 4.99, N 15.76; found: C 70.35, H 4.65, N 15.70.

#### 4.8. General procedure for Huisgen–Meldal–Sharpless [3+2] cycloaddition performed on oligonucleotides in aqueous solution with 1-azidomethylpyrene **10**

To a ss oligonucleotide, CuSO<sub>4</sub>·TBTA (1:1) ligand complex (50 μL of a 20 mM stock solution in H<sub>2</sub>O/DMSO/*t*-BuOH, 4:3:1), 1-azidomethylpyrene (**10**, 60 μL of a 20 mM stock solution in H<sub>2</sub>O/dioxane/DMSO, 1:1:1), tris-(carboxyethyl)phosphine (TCEP, 50 μL of a 20 mM stock solution in water), NaHCO<sub>3</sub> (50 μL of 200 mM stock solution in water), and DMSO (50 μL) were added, and the reaction mixture was stirred at room temperature for 12 h. The reaction mixture was concentrated in a speed vac and dissolved in 500 μL bidistilled water and centrifuged for 30 min at 14,000 rpm. The residue was further purified by reversed-phase HPLC with the gradient: 0–3 min 10–15% B in A, 3–15 min 15–50% B in A,

15–20 min 50–10% B in A, 20–25 min 10% B in A, flow rate 0.8 cm<sup>3</sup> min<sup>-1</sup>. The molecular masses of the oligonucleotides were determined by MALDI-TOF or LC-ESI-TOF mass spectrometry (Table S1, Supplementary data).

#### 4.9. Fluorescence studies

Fluorescence spectra of nucleoside 'click' conjugates **1** and **2** were measured in methanol. For solubility reasons, the nucleosides were first dissolved in 1 mL of DMSO and then diluted with 99 mL of methanol. All measurements were performed with identical concentrations of 6.8 μM. Fluorescence spectra of ss oligonucleotide 'click' conjugates and their duplexes were measured in 1 M NaCl, 100 mM MgCl<sub>2</sub>, and 60 mM Na-cacodylate buffer (pH 7.0). All measurements were performed with identical concentrations, i.e., 2 μM for ss oligonucleotides and 2 μM+2 μM for ds oligonucleotides. The extinction coefficients ε<sub>260</sub> of nucleosides used to calculate the oligonucleotide concentration were: dA 15,400, dG 11,700, dT 8800, dC 7300, **1** 19,300, **2** 35,100, **3** 26,000 and **4** 34,100. A 20% hyperchromicity was taken into account for all oligonucleotides.

#### Acknowledgements

We thank Mr. N. Q. Tran for the oligonucleotide synthesis and Dr. R. Thiele from Roche Diagnostics, Penzberg for the measurement of the MALDI spectra. We also thank Dr. P. Leonard and Dr. S. Budow for their continuous support throughout the preparation of the manuscript and appreciate critical reading of the manuscript by Mr. S. S. Pujari. Financial support by ChemBiotech, Münster, Germany, is highly appreciated.

#### Supplementary data

Structures of phosphoramidites, molecular masses of oligonucleotides, <sup>1</sup>H–<sup>13</sup>C-coupling constants, HPLC profiles of post-synthetic labeled oligonucleotides, UV/vis and fluorescence spectra of oligonucleotide pyrene conjugates, melting curves of oligonucleotide duplexes, <sup>1</sup>H NMR, <sup>13</sup>C NMR, DEPT-135 NMR and <sup>1</sup>H–<sup>13</sup>C gated-decoupled spectra of all new compounds **1**, **2**, **5**, **6** and **7**, and <sup>31</sup>P NMR spectrum of phosphoramidite **8**. Supplementary data related to this article can be found at <http://dx.doi.org/10.1016/j.tet.2013.03.054>.

#### References and notes

- (a) Sinkeldam, R. W.; Greco, N. J.; Tor, Y. *Chem. Rev.* **2010**, *110*, 2579; (b) Gonçalves, M. S. T. *Chem. Rev.* **2009**, *109*, 190.
- (a) Wang, C.; Wu, C.; Chen, Y.; Song, Y.; Tan, W.; Yang, C. *J. Curr. Org. Chem.* **2011**, *15*, 465; (b) Østergaard, M. E.; Hrdlicka, P. J. *Chem. Soc. Rev.* **2011**, *40*, 5771.
- (a) Briks, J. B. In *Photophysics of Aromatic Molecules*; Wiley-Interscience: London, UK, 1970; pp 301–370; (b) Winnik, F. M. *Chem. Rev.* **1993**, *93*, 587.
- Ingale, S. A.; Seela, F. J. *Org. Chem.* **2012**, *77*, 9352.
- (a) Sau, S. P.; Kumar, T. S.; Hrdlicka, P. J. *Org. Biomol. Chem.* **2010**, *8*, 2028; (b) Astakhova, I. V.; Malakhov, A. D.; Stepanova, I. A.; Ustinov, A. V.; Bondarev, S. L.; Paramonov, A. S.; Korshun, V. A. *Bioconjug. Chem.* **2007**, *18*, 1972.
- (a) Hrdlicka, P. J.; Babu, B. R.; Sørensen, M. D.; Wengel, J. *Chem. Commun.* **2004**, 1478; (b) Hrdlicka, P. J.; Kumar, T. S.; Wengel, J. *Chem. Commun.* **2005**, 4279.
- (a) Langenegger, S. M.; Häner, R. *Chem. Commun.* **2004**, 2792; (b) Werder, S.; Malinovskii, V. L.; Häner, R. *Org. Lett.* **2008**, *10*, 2011; (c) Malinovskii, V. L.; Samain, F.; Häner, R. *Angew. Chem., Int. Ed.* **2007**, *46*, 4464.
- (a) Gao, J.; Strässler, C.; Tahmassebi, D.; Kool, E. T. *J. Am. Chem. Soc.* **2002**, *124*, 11590; (b) Wilson, J. N.; Teo, Y. N.; Kool, E. T. *J. Am. Chem. Soc.* **2007**, *129*, 15426.
- Seo, Y. J.; Rhee, H.; Joo, T.; Kim, B. H. *J. Am. Chem. Soc.* **2007**, *129*, 5244.
- (a) Nakamura, M.; Ohtoshi, Y.; Yamana, K. *Chem. Commun.* **2005**, 5163; (b) Nakamura, M.; Shimomura, Y.; Ohtoshi, Y.; Sasa, K.; Hayashi, H.; Nakano, H.; Yamana, K. *Org. Biomol. Chem.* **2007**, *5*, 1945; (c) Nakamura, M.; Murakami, Y.; Sasa, K.; Hayashi, H.; Yamana, K. *J. Am. Chem. Soc.* **2008**, *130*, 6904; (d) Nakamura, M.; Fukuda, M.; Takada, T.; Yamana, K. *Org. Biomol. Chem.* **2012**, *10*, 9620.
- (a) Seela, F.; Ingale, S. A. *J. Org. Chem.* **2010**, *75*, 284; (b) Ingale, S. A.; Pujari, S. S.; Sirivolu, V. R.; Ding, P.; Xiong, H.; Mei, H.; Seela, F. *J. Org. Chem.* **2012**, *77*, 188.

12. (a) Huisgen, R.; Szeimies, G.; Möbius, L. *Chem. Ber.* **1967**, *100*, 2494; (b) Tornøe, C. W.; Christensen, C.; Meldal, M. *J. Org. Chem.* **2002**, *67*, 3057; (c) Rostovtsev, V. V.; Green, L. G.; Fokin, V. V.; Sharpless, K. B. *Angew. Chem., Int. Ed.* **2002**, *41*, 2596.
13. (a) Sirivolu, V. R.; Chittepu, P.; Seela, F. *ChemBioChem* **2008**, *9*, 2305; (b) Seela, F.; Xiong, H.; Budow, S. *Tetrahedron* **2010**, *66*, 3930.
14. Seela, F.; Sirivolu, V. R.; Chittepu, P. *Bioconjug. Chem.* **2008**, *19*, 211.
15. Wanninger-Weiß, C.; Valis, L.; Wagenknecht, H.-A. *Bioorg. Med. Chem.* **2008**, *16*, 100.
16. (a) Manoharan, M.; Tivel, K. L.; Zhao, M.; Nafisi, K.; Netzel, T. L. *J. Phys. Chem.* **1995**, *99*, 17461; (b) Seo, Y. J.; Ryu, J. H.; Kim, B. H. *Org. Lett.* **2005**, *7*, 4931; (c) Sau, S. P.; Hrdlicka, P. J. *J. Org. Chem.* **2012**, *77*, 5.
17. (a) Okamoto, A.; Kanatani, K.; Saito, I. *J. Am. Chem. Soc.* **2004**, *126*, 4820; (b) Yamana, K.; Zako, H.; Asazuma, K.; Iwase, R.; Nakano, H.; Murakami, A. *Angew. Chem., Int. Ed.* **2001**, *40*, 1104; (c) Yamana, K.; Iwase, R.; Furutani, S.; Tsuchida, H.; Zako, H.; Yamaoka, T.; Murakami, A. *Nucleic Acids Res.* **1999**, *27*, 2387; (d) Nakamura, M.; Fukunaga, Y.; Sasa, K.; Ohtoshi, Y.; Kanaori, K.; Hayashi, H.; Nakano, H.; Yamana, K. *Nucleic Acids Res.* **2005**, *33*, 5887; (e) Hrdlicka, P. J.; Babu, B. R.; Sørensen, M. D.; Harrit, N.; Wengel, J. *J. Am. Chem. Soc.* **2005**, *127*, 13293; (f) Østergaard, M. E.; Kumar, P.; Baral, B.; Guenther, D. C.; Anderson, B. A.; Ytreberg, F. M.; Deobald, L.; Paszczyński, A. J.; Sharma, P. K.; Hrdlicka, P. J. *Chem.—Eur. J.* **2011**, *17*, 3157.
18. Kumar, P.; Shaikh, K. I.; Jørgensen, A. S.; Kumar, S.; Nielsen, P. J. *Org. Chem.* **2012**, *77*, 9562.
19. (a) Mayer-Enthart, E.; Wagenknecht, H.-A. *Angew. Chem., Int. Ed.* **2006**, *45*, 3372; (b) Barbaric, J.; Wagenknecht, H.-A. *Org. Biomol. Chem.* **2006**, *4*, 2088.
20. (a) Dohno, C.; Saito, I. *ChemBioChem* **2005**, *6*, 1075; (b) Seela, F.; Jiang, D.; Budow, S. *ChemBioChem* **2010**, *11*, 1443; (c) Ming, X.; Seela, F. *Chem.—Eur. J.* **2012**, *18*, 9590.